Electronic Supplementary Material (ESI) for Sustainable Energy & Fuels.

Supplementary Information

Interface engineering for light-driven water oxidation: Unravelling the passivating and catalytic mechanism in $BiVO_4$ overlayers †

Guiji Liu,[a,b] Johanna Eichhorn, [a,b] Chang-Ming Jiang, [a,b] Mary C. Scott, [e,f] Lucas H. Hess, [a,b] John M. Gregoire,[c] Joel A. Haber,[c] Ian D. Sharp [a,b,d] Francesca M. Toma,* [a,b]

a. Joint Center for Artificial Photosynthesis, Lawrence Berkeley National Laboratory, 1 Cyclotron Road, Berkeley, California 94720, USA.

b. Chemical Sciences Division, Lawrence Berkeley National Laboratory, 1 Cyclotron Road, Berkeley, California 94720, USA.

c. Joint Center for Artificial Photosynthesis, California Institute of Technology; Pasadena, CA 91125, USA.

d. Walter Schottky Institut and Physik Department, Technische Universität München, Am Coulombwall 4, 85748 Garching, Germany.

e. Department of Materials Science and Engineering, University of California Berkeley, Berkeley, USA.

f. National Center for Electron Microscopy, Molecular Foundry, Lawrence Berkeley National Laboratory, Berkeley, USA

Email: fmtoma@lbl.gov

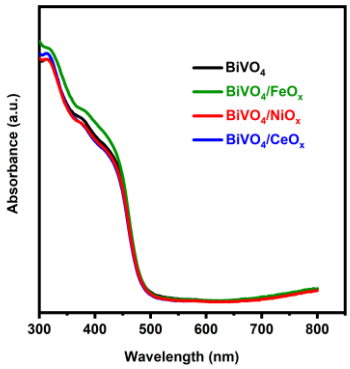

Figure S1 UV-Vis spectra of $BiVO_4$, $BiVO_4/FeO_x$, $BiVO_4/NiO_x$ and $BiVO_4/CeO_x$.

	Sample	J_0 @ 1.23 V RHE with H_2O_2 (mA cm^{-2})	J_1 @ 1.23 V RHE (mA cm^{-2})	J_1/J_0@1.23 V RHE (%)
1	$BiVO_4$	1.5	0.7	48
2	$BiVO_4/CeO_x$	2.2	0.6	27
3	$BiVO_4/FeO_x$	1.9	1.3	67
4	$BiVO_4/NiO_x$	1.9	1.5	79

Table S1 Summary of photocurrent densities of $BiVO_4$, $BiVO_4/CeO_x$, $BiVO_4/FeO_x$ and $BiVO_4/NiO_x$ photoanodes at 1.23 V in 0.1 M NaOH solutions with or without H_2O_2 under AM 1.5G simulated sunlight at 100 mW cm^{-2}. Data was taken from Fig. 1a and b in the main text.

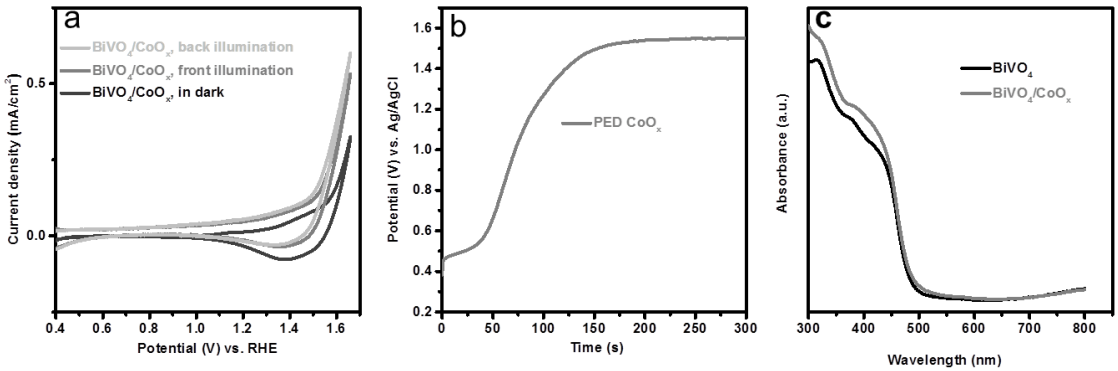

Figure S2 a Cyclic voltammograms of $BiVO_4/CoO_x$ photoanodes in dark under front and back illuminations (AM 1.5G simulated sunlight at 100 mW cm^{-2}); b Potential-time profile of depositing CoO_x on $BiVO_4$ with PED under AM 1.5G simulated sunlight at 100 mW cm^{-2}; c UV-Vis spectra of $BiVO_4$ and $BiVO_4/CoO_x$.

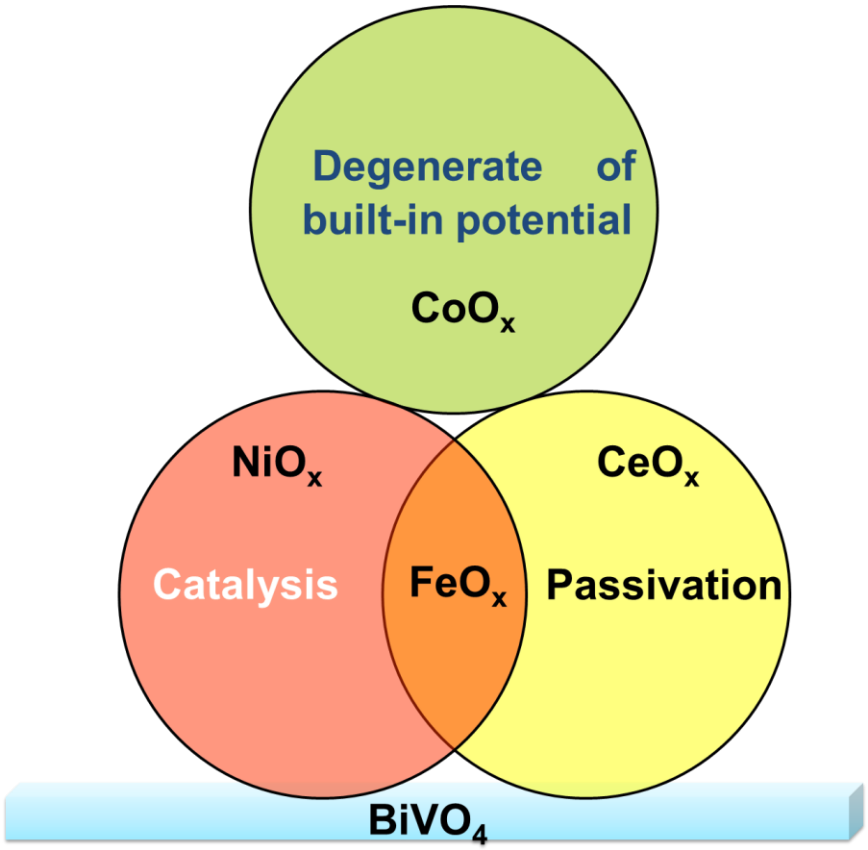

Figure S3 Schematic illustration of individual role of the metal oxide overlayers.

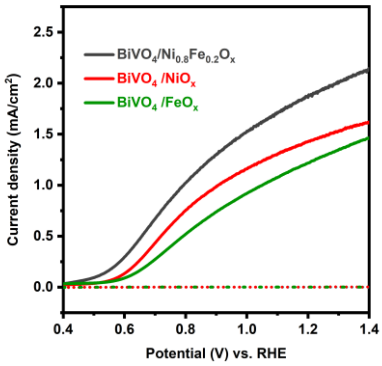

Figure S4 Current-potential curves of $BiVO_4/Ni_{0.8}Fe_{0.2}O_x$, $BiVO_4/NiO_x$ and $BiVO_4/FeO_x$ photoanodes under AM 1.5G simulated sunlight at 100 mW cm^{-2} in 0.1 M NaOH aqueous solution (pH = 13).

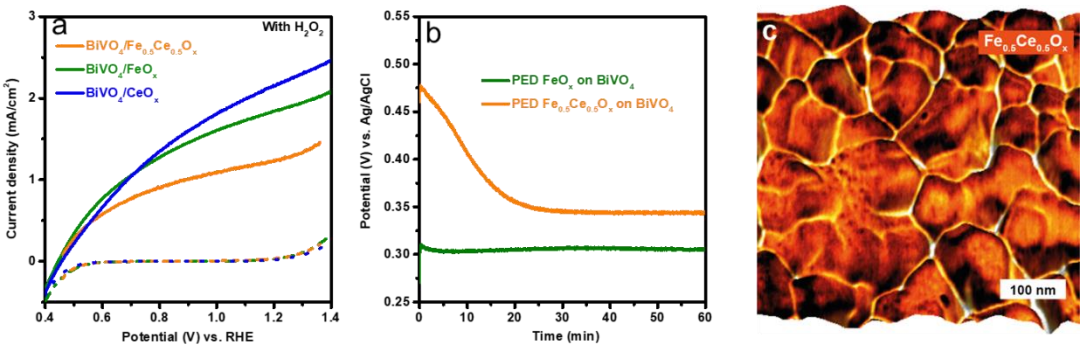

Figure S5 a Current-potential curves of $BiVO_4/FeO_x$, $BiVO_4/CeO_x$ and $BiVO_4/Fe_{0.5}Ce_{0.5}O_x$ photoanodes in dark (dashed lines) and under AM 1.5G simulated sunlight at 100 mW cm^{-2} in 0.1 M NaOH + H_2O_2 aqueous solution (pH = 13); b Potential-time profiles of depositing FeO_x and $Fe_{0.5}Ce_{0.5}O_x$ on $BiVO_4$ with PED under AM 1.5G simulated sunlight at 100 mW cm^{-2}; c Overlay images of the sample topography and the corresponding adhesion maps for $BiVO_4/Fe_{0.5}Ce_{0.5}O_x$. $Fe_{0.5}Ce_{0.5}O_x$ was deposited with mixing 0.05 M iron nitrate (III) nonahydrate and 0.05 M cerium nitrate (III) hexahydrate into in total 0.1 M metal nitrate solution as plating solution.

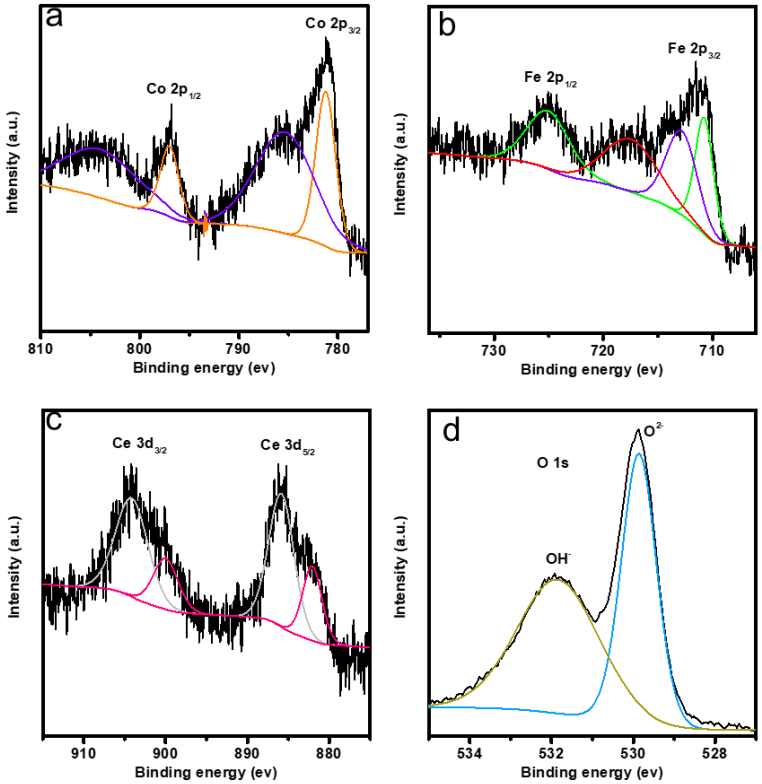

Figure S6 XPS spectra of a Co2p, b Fe 2p, c Ce 3d and d O 1s for $BiVO_4/Co_{0.4}Fe_{0.1}Ce_{0.5}O_x$.

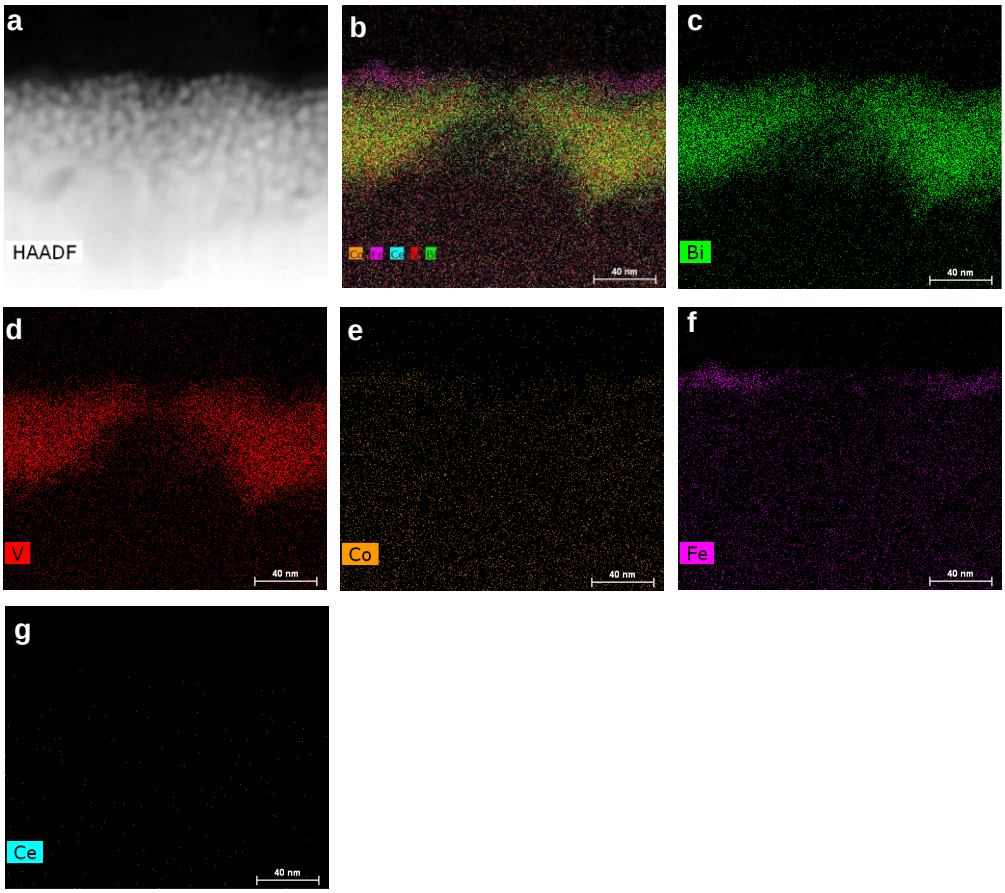

Figure S7 a STEM image of $BiVO_4/Co_{0.4}Fe_{0.1}Ce_{0.5}O_x$; b Overlap of multiple EDS elemental mapping of Co, Fe, Ce, V, Bi for $BiVO_4/Co_{0.4}Fe_{0.1}Ce_{0.5}O_x$; individual mapping of c Bi, d V, e Co, f Fe, g Ce for $BiVO_4/Co_{0.4}Fe_{0.1}Ce_{0.5}O_x$.

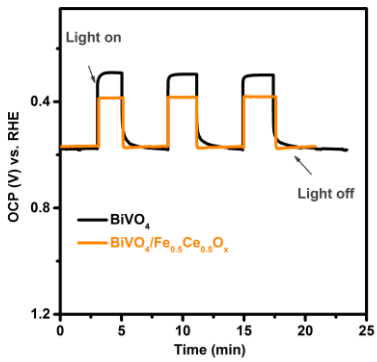

Figure S8 OCP profile $BiVO_4/Fe_{0.5}Ce_{0.5}O_x$ and $BiVO_4$ photoanodes under chopped AM 1.5G simulated sunlight at 100 mW cm^{-2} in 0.1 M NaOH aqueous solution (pH = 13).

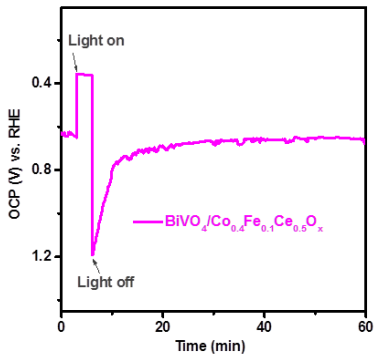

Figure S9 OCP profile $BiVO_4/Co_{0.4}Fe_{0.1}Ce_{0.5}O_x$ photoanodes under chopped AM 1.5G simulated sunlight at 100 mW cm^{-2} in 0.1 M NaOH aqueous solution (pH = 13).

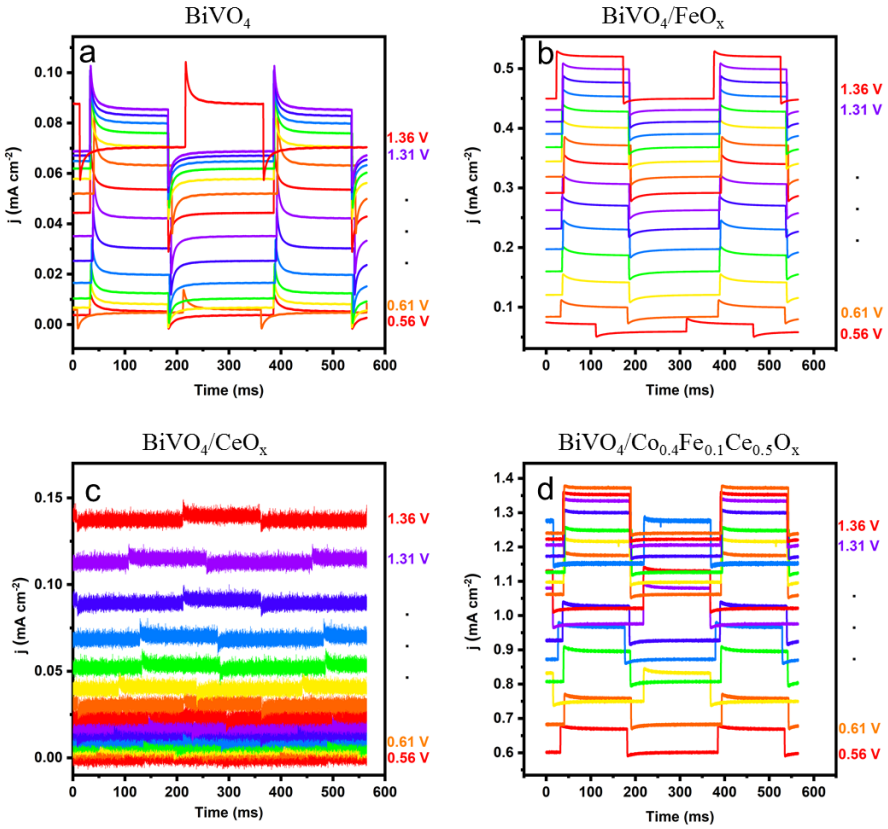

Figure S10 Transient photocurrent responses measured from a $BiVO_4$, $BiVO_4/FeO_x$, $BiVO_4/CeO_x$ and $BiVO_4/Co_{0.4}Fe_{0.1}Ce_{0.5}O_x$ in 0.1 M NaOH aqueous solution (pH = 13) at 0.56-1.36 V RHE.

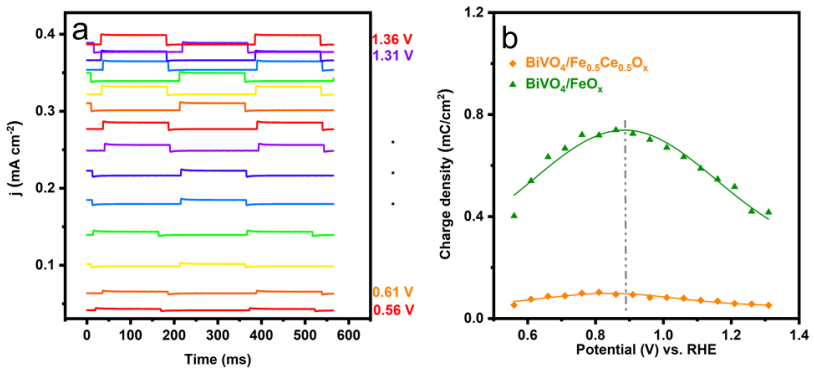

Figure S11 a Transient photocurrent responses measured from a $BiVO_4/Fe_{0.5}Ce_{0.5}O_x$ in 0.1 M NaOH aqueous solution (pH = 13) at 0.56-1.36 V RHE; b Accumulated charge versus potential curves obtained from transient photocurrent data of $BiVO_4/Fe_{0.5}Ce_{0.5}O_x$, $BiVO_4/FeO_x$ is used as comparison.

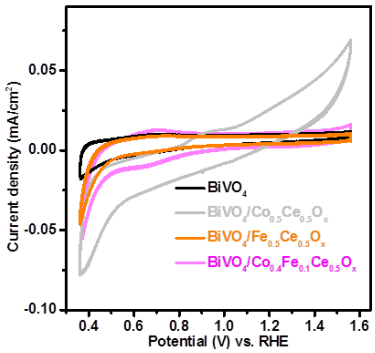

Figure S12 Cyclic voltammograms of $BiVO_4$, $BiVO_4/Co_{0.5}Ce_{0.5}O_x$, $BiVO_4/Fe_{0.5}Ce_{0.5}O_x$ and $BiVO_4/Co_{0.4}Fe_{0.1}Ce_{0.5}O_x$ electrodes in dark in 0.1 M NaOH aqueous solution (pH = 13) with three cycles, scan rate: 500 mV/s. $Co_{0.5}Ce_{0.5}O_x$ was deposited with mixing 0.05 M cobalt (II) nitrate hexahydrate and 0.05 M cerium nitrate (III) hexahydrate into in total 0.1 M metal nitrate solution as plating solution.

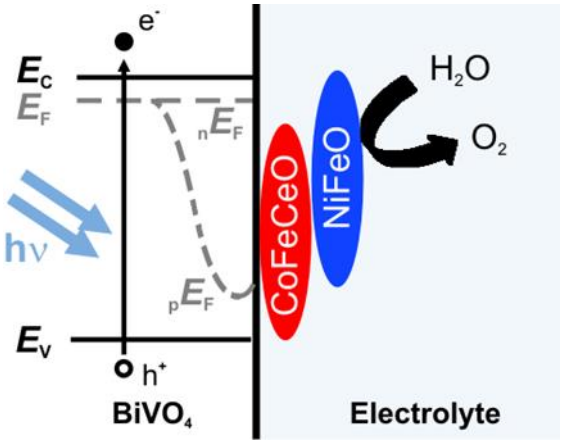

Figure S13 Schematic illustration of integrated $BiVO_4/Co_{0.4}Fe_{0.1}Ce_{0.5}O_x/Ni_{0.8}Fe_{0.2}O_x$ photoanode. $Ni_{0.8}Fe_{0.2}O_x$ catalyst was deposited atop to utilize surface-reaching holes that were collected by

$Co_{0.4}Fe_{0.1}Ce_{0.5}O_x$ overlayer from $BiVO_4$ light absorber for water oxidation. E_c and E_v represent conduction band and valence band position of $BiVO_4$, respectively. E_F represents Fermi level of $BiVO_4$ in dark, while ${}_pE_F$ and ${}_nE_F$ are referred to quasi-Fermi levels for holes and electrons respectively under illumination.

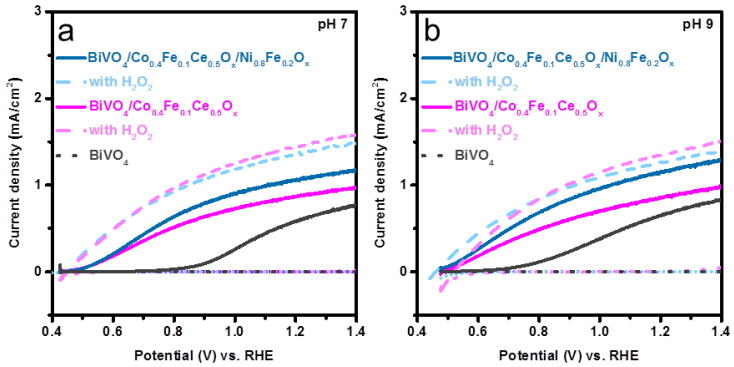

Figure S14 Current-potential curves of $BiVO_4$, $BiVO_4/Co_{0.4}Fe_{0.1}Ce_{0.5}O_x$, and $BiVO_4/Co_{0.4}Fe_{0.1}Ce_{0.5}O_x/Ni_{0.8}Fe_{0.2}O_x$ photoanodes in dark (dotted lines) under AM 1.5G simulated sunlight at 100 mW cm^{-2} photoanodes in a 0.1 M KPi aqueous solution (pH = 7) and b 0.1 M NaBi aqueous solution (pH = 9), comparing to current-potential curves of $BiVO_4/Co_{0.4}Fe_{0.1}Ce_{0.5}O_x/Ni_{0.8}Fe_{0.2}O_x$ and $BiVO_4/Co_{0.4}Fe_{0.1}Ce_{0.5}O_x$ photoanodes (dashed lines) in a 0.1 M KPi + H_2O_2 aqueous solution (pH = 7) and b 0.1 M NaBi + H_2O_2 aqueous solution (pH = 9).

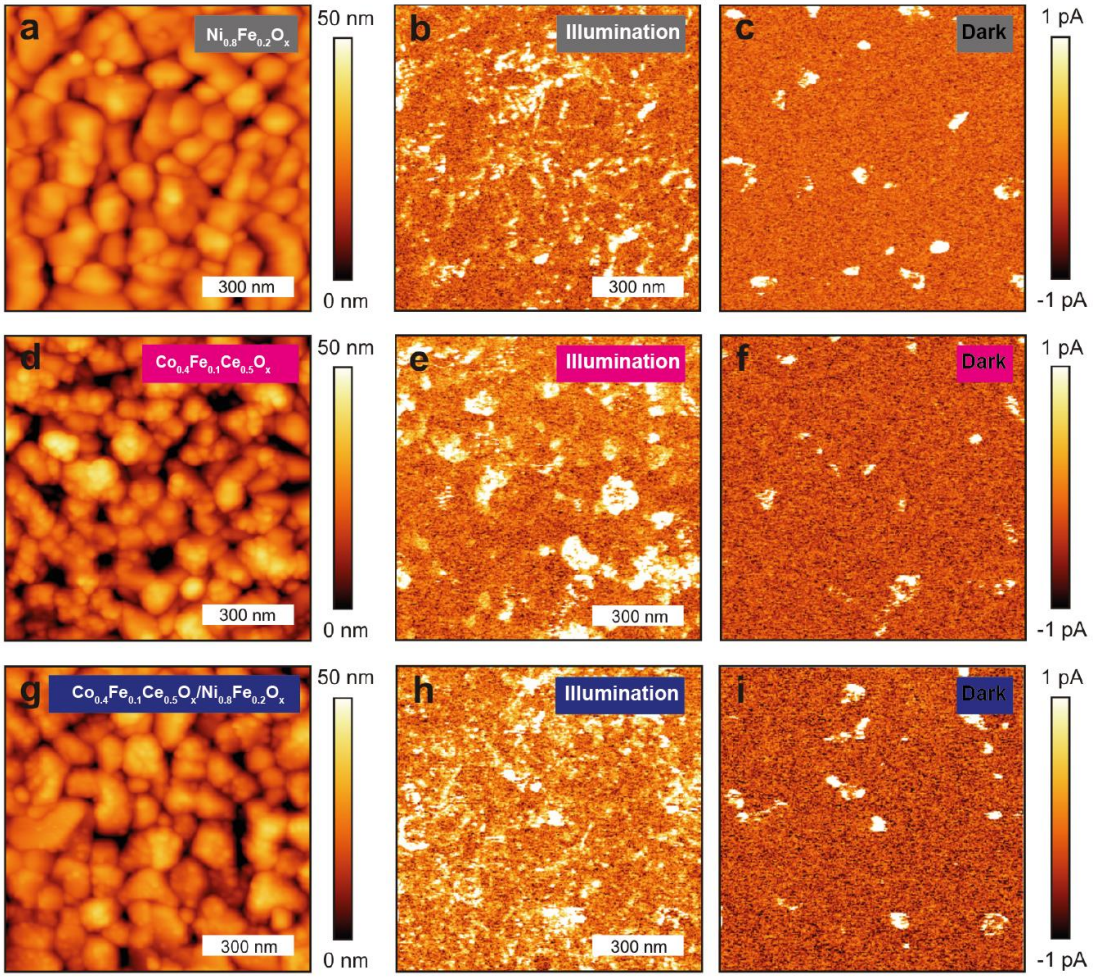

Figure S15 Topographic and current maps collected for $BiVO_4/Ni_{0.8}Fe_{0.2}O_x$ (a, b, c), $BiVO_4/Co_{0.4}Fe_{0.1}Ce_{0.5}O_x$ (d, e, f) and $BiVO_4/Co_{0.4}Fe_{0.1}Ce_{0.5}O_x/Ni_{0.8}Fe_{0.2}O_x$ (g, h, i).

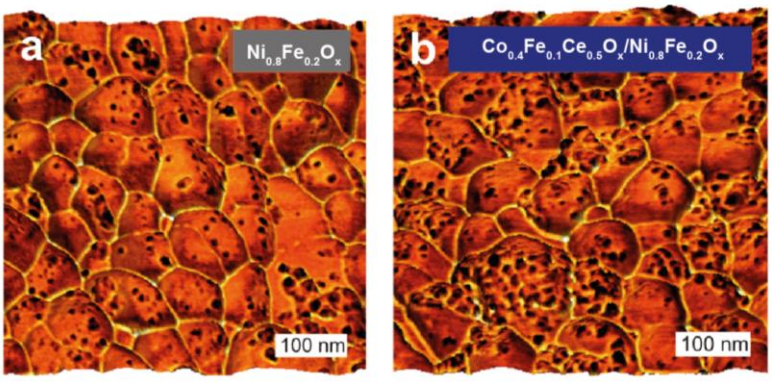

Figure S16 The overlay of topography & adhesion images of a $BiVO_4/Ni_{0.8}Fe_{0.2}O_x$ and b $BiVO_4/Co_{0.4}Fe_{0.1}Ce_{0.5}O_x/Ni_{0.8}Fe_{0.2}O_x$.